Journal of Structural Geology 30 (2008) 1024–1033

Contents lists available at ScienceDirect

Journal of Structural Geology

journal homepage: www.elsevier.com/locate/jsg

Rotated garnets: a mechanism to explain the high frequency of inclusion trail curvature angles around 90° and 180°

Rudolph A.J. Trouw [a,*], Felipe M. Tavares [a], Martin Robyr [b]

[a] Departamento de Geologia, I.GEO, UFRJ, Ilha do Fundão, 21949-900, Rio de Janeiro, Brazil
[b] Geological Science Department, The University of Texas at Austin,1 University Station C1100, Austin, TX 78712-0254, USA

ARTICLE INFO

Article history:
Received 25 April 2007
Received in revised form 16 April 2008
Accepted 28 April 2008
Available online 14 May 2008

Keywords:
Rotated garnets
Spiral shaped inclusion trails
Preferential growth
Pulsating rotation

ABSTRACT

This paper presents numerical data from garnets with inclusion trail curvature angles of up to 260°. Three hundred and twenty-five garnets were studied from an outcrop of greenschist facies phyllite in southern Minas Gerais State, Brazil. Apart from the inclusion trail curvature angle α, also the aspect ratio R and the angle between the long axis of the garnets and the foliation, β, were measured. The results show a remarkable concentration of α at 180° and a minor one at 90°. R varies between 1 and 2 showing that the garnets deviate from sphericity and β shows that all garnets have their long axis in the "forward rotated" quadrant, supporting the rotational interpretation. A model is proposed to explain the concentrations of α, based on preferential growth of the garnets into the mica rich strain caps, orthogonal to the foliation, causing elongated crystals that, because of their shape and position would experience accelerated rotation until relatively stable positions with their long axes parallel to the foliation would be attained. Renewed growth, again into the mica-rich strain caps, orthogonal to the foliation would first restore the spherical shape and then produce an elongated shape, again perpendicular to the foliation, forcing a repetition of the process. It is concluded that this model is capable of explaining the concentration of α in multiples of 90°, in a rotational model, where this concentration was considered earlier as an argument in favor of the non-rotational model.

1. Introduction

Garnets with spiral shaped inclusion trails have been interpreted as rotational or non-rotational (see reviews by Johnson, 1993a, 1999a,b; Jiang and Williams, 2004; Passchier and Trouw, 2005). Although there are indications that both models are at least to some extent feasible and may operate in nature, it seems to be hard to define geometric criteria to distinguish between them (Johnson, 1999b). In many cases it is therefore not clear which one of the mechanisms operated.

Several arguments have been put forward in favor of either of the two mechanisms (Johnson, 1993a, 1999b; Williams and Jiang, 1999; Jiang, 2001). The importance of reference frames was especially emphasized by Jiang and Williams (2004). One of the arguments in favor of the non-rotational model is the fact that inclusion trail curvature angles cluster in multiples of 90° (Johnson, 1993a, his Fig. 12). In the non-rotational model (e.g. Bell and Johnson, 1989) this clustering could be explained by nucleation pulses at the initiation of each new deformation phase. In the rotational model it is not obvious why new porphyroblasts would nucleate after older ones rotated about 90°, 180°, 270° etc.

This paper presents numerical data from samples of a well-studied area in southern Minas Gerais State, Brazil, where general shear sense, metamorphic history and the succession of deformation phases are satisfactorily understood. The model of progressive rotation of syntectonically growing garnets is favored for several reasons, explained below. A remarkable concentration of inclusion curvature angles around 90° and 180° is present. A model is proposed to explain this, based on the elongated shape of most of the garnets that would favor rotation to relatively stable positions with the long axes at a small angle or parallel to the foliation.

2. Geology of the study area

The samples are taken from a railway cut at about 2 km south of the city of Itumirim, southern Minas Gerais State, Brazil (Fig. 1). The outcrop is composed of phyllite with intercalated quartzite belonging to the Campestre Unit of the Neoproterozoic Andrelândia Megasequence (Paciullo et al., 2000).

The phyllite contains muscovite, quartz, chloritoid, garnet, chlorite, locally some staurolite and opaque minerals, principally graphite, as very small grains included in other minerals. The

* Corresponding author. Tel.: +55 21 25989482.
E-mail address: rajtrouw@hotmail.com (R.A.J. Trouw).

0191-8141/$ – see front matter © 2008 Elsevier Ltd. All rights reserved.
doi:10.1016/j.jsg.2008.04.011

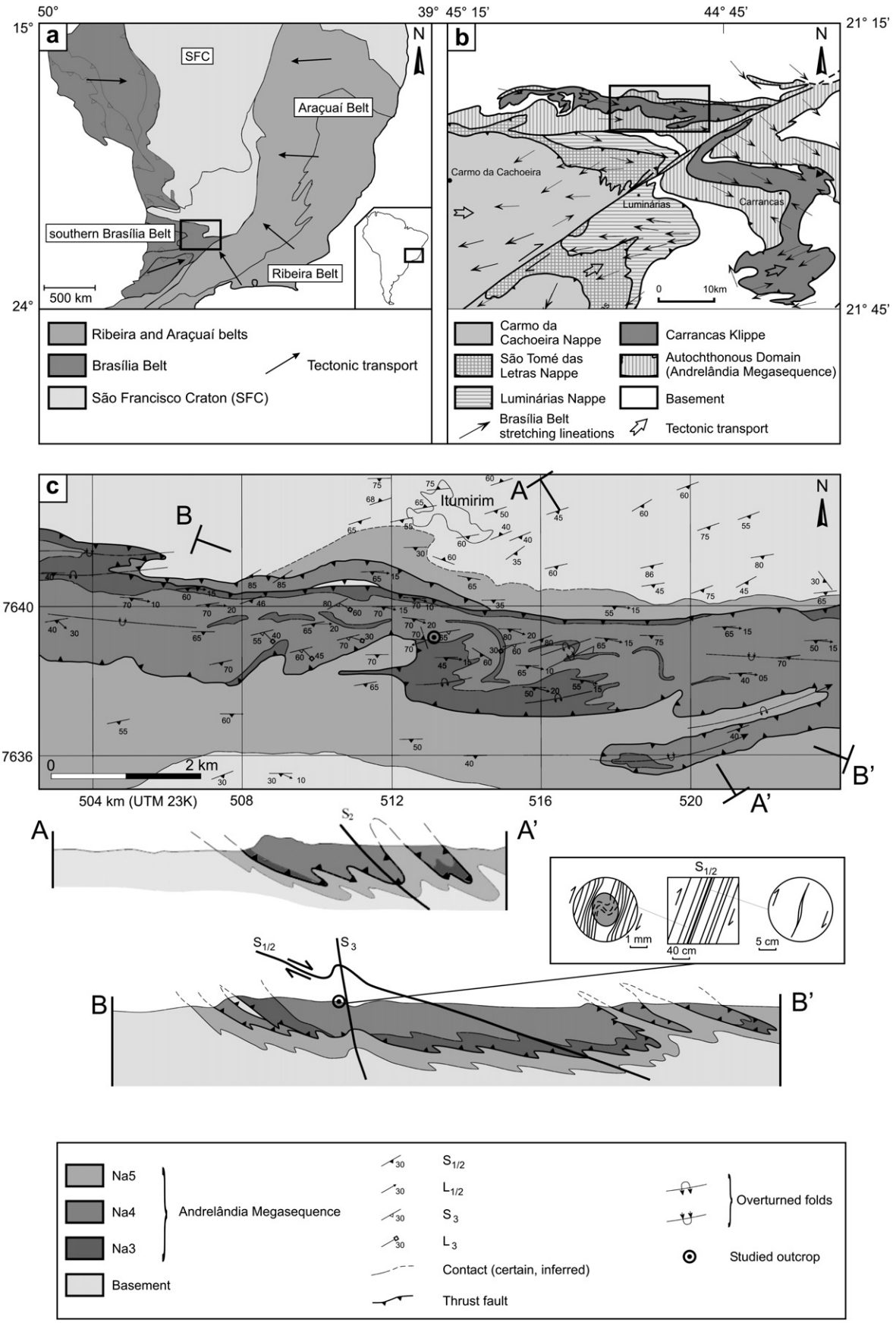

Fig. 1. Geological setting of the studied outcrop. (a) Location of the Brasília Belt in Brazil; (b) tectonic map of the southern part of the Brasília Belt, showing nappes, stretching lineations and tectonic transport; (c) geological map of the area south of Itumirim, with the studied outcrop indicated on the map and on section B–B′.

metamorphic grade is upper greenschist facies (Fig. 1b), grading to amphibolite facies, as indicated by the association: garnet + chloritoid + chlorite + muscovite + quartz and locally staurolite. Biotite is not present because of inadequate chemical composition.

The outcrop is situated in a klippe, the Carrancas Klippe (Fig. 1a; Trouw et al., 2000), that is tightly folded. The klippe is part of a stack of nappes, the Andrelândia Nappe Complex, that constitute the southern Brasília Belt of Neoproterozoic age (Fig. 1a; Campos Neto and Caby, 1999, 2000; Trouw et al., 2000). The overall sense of shear in the nappes is top to the east and the metamorphic grade increases from lower greenschist facies in the autochthon to granulite facies in the upper nappes. Deformational structures were grouped in three sets, ascribed to three successive deformation phases, D_1, D_2 and D_3. D_1 and D_2 are related phases, responsible for the main, flat lying cleavage, associated with tight to isoclinal folds with approximately E–W axes, parallel to a conspicuous aggregate lineation, interpreted as a stretching lineation. These phases also generated the nappes through eastward thrust movements, documented by numerous shear sense indicators such as asymmetric mica and foliation fish, C/S fabrics, oblique foliation etc. (Campos Neto and Caby, 1999, 2000; Trouw et al., 2000). Locally, D_1 and D_2 can be separated by interference structures such as refolded folds or crenulation cleavage, but at many sites, including the outcrop considered here, only a single slaty cleavage is present and interference patterns of refolding are lacking. D_1 and D_2 are therefore interpreted as representing a single progressive deformation, related to continental collision that led to eastwards extrusional mass movement, including nappe formation. At local constriction sites folding and refolding generated D_1 and D_2 structures, but at many other sites the total deformation resulted in a single slaty cleavage, labeled $S_{1/2}$ with accompanying E–W stretching lineation, $L_{1/2}$. D_3 folded the earlier structures, with axial planes dipping steeply to W–SW and subhorizontal to shallow N–S to NE–SW axes. D_3 folds vary in tightness from gentle to tight, and generally no penetrative S_3 cleavage is developed.

The slaty cleavage in the samples (Figs. 2, 3) is $S_{1/2}$. At the studied outcrop it dips about 70° to the west (260/72) and the attitude of the stretching lineation $L_{1/2}$ is approximately down dip. This steep attitude is anomalous and is due to the fact that the outcrop is situated in the short limb of a hectometric D_3 fold (Fig. 1c). The sense of apparent rotation, assuming that the garnets rotated with respect to a stable matrix foliation, is coherent with the regional shear sense that is top to the east, after back-rotation of the steep D_3 limb to the original flat lying position (Figs. 1, 3).This shear sense is also confirmed by independent shear sense indicators at the same outcrop, such as foliation fish, composed of a large number of muscovite grains (Fig. 3f) of the same size and crystal habit as the muscovites in the matrix around the garnets.

In thin sections incipient D_3 crenulation with axial planes at high angles or orthogonal to $S_{1/2}$ can be observed locally (e.g. Figs. 2, 3a,c,e). This deformation is clearly post-garnet growth and has no relation to the rotated garnets, except for the fact that the garnets probably acted as favorable nucleation sites for D_3 crenulation, because $S_{1/2}$ was already deflected around them.

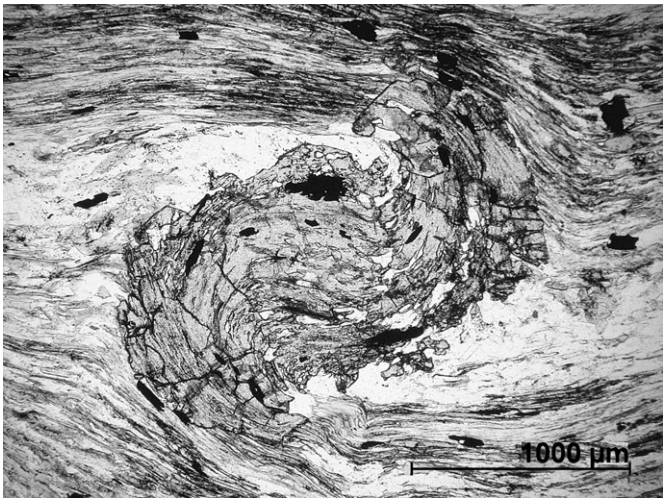

Fig. 2. Typical example of the studied garnets; note the continuity between S_i and S_e ($= S_{1/2}$) and the similar grain size of the inclusions within the garnet and the grains in the matrix. Note also the elongated shape of the garnet that seems to have grown preferentially into its strain caps. The inclusion trail curvature angle α is about 180°, the aspect ratio R is 1.8 and the angle β (see Fig. 4 and text) is 40°. In the central lower part of the photomicrograph D_3 crenulation is visible.

3. Interpretation of garnet growth

The garnets are interpreted as having grown syntectonically during $D_{1/2}$ because of their inclusion patterns and the slight deviation of $S_{1/2}$ around them (Passchier and Trouw, 2005, their Fig. 7.9).

The garnets are also interpreted as rotational with respect to the surrounding cleavage based on the following arguments:

- the continuation of cleavage planes (Figs. 2, 3) outside (S_e) and inside the garnets (S_i), together with the similar size of cleavage forming minerals suggests that they represent the same cleavage;
- no remnant crenulations were found in the strain shadows, as would be expected in the non-rotational model, where successive crenulation cleavages are erased in the matrix, but could survive in protected areas in the strain shadows;
- there is no evidence or indication in the regional tectonic evolution to justify more than two deformational phases until the end of the garnet growth, whereas the non-rotational model would require at least four orthogonal phases to explain the spiral shaped inclusion trail angles of up to 260°;
- according to the rotational model the rotation would be coherent with the regional sense of shear determined by other shear sense criteria, whereas the non-rotational model would require opposite shear sense, with top to the west movements, which in the regional context does not make sense;
- independent shear sense indicators, like asymmetric foliation fish (Fig. 3f) are present in the same outcrop, indicating the same sense of shear (top to the west) as the rotational model predicts. One could argue that the foliation fish did not necessarily form contemporaneously with the garnets. However, the inclusion pattern continuous with S_e shows that no significant shear movement took place after garnet growth, excluding formation of the fish at this stage. It also seems unlikely that the fish formed before garnet growth, in a shear regime with opposite shear sense, and remained intact during garnet growth;
- as shown below, the long axes of elongated garnets are always situated in the "forward rotated" quadrant, with relation to the rotational model. This is difficult to match with the non-rotational model where the sense of shear would be opposite and the long axes would be in the "backwards rotated" quadrant (see also Section 6).

4. Measured data

Several oriented samples were taken from the studied outcrop and 22 thin sections were selected, in which a total of 325 garnets with spiral shaped inclusion patterns were studied. All sections are orthogonal to the $S_{1/2}$ foliation and parallel to the $L_{1/2}$ stretching lineation. We are aware that selected median sections would be

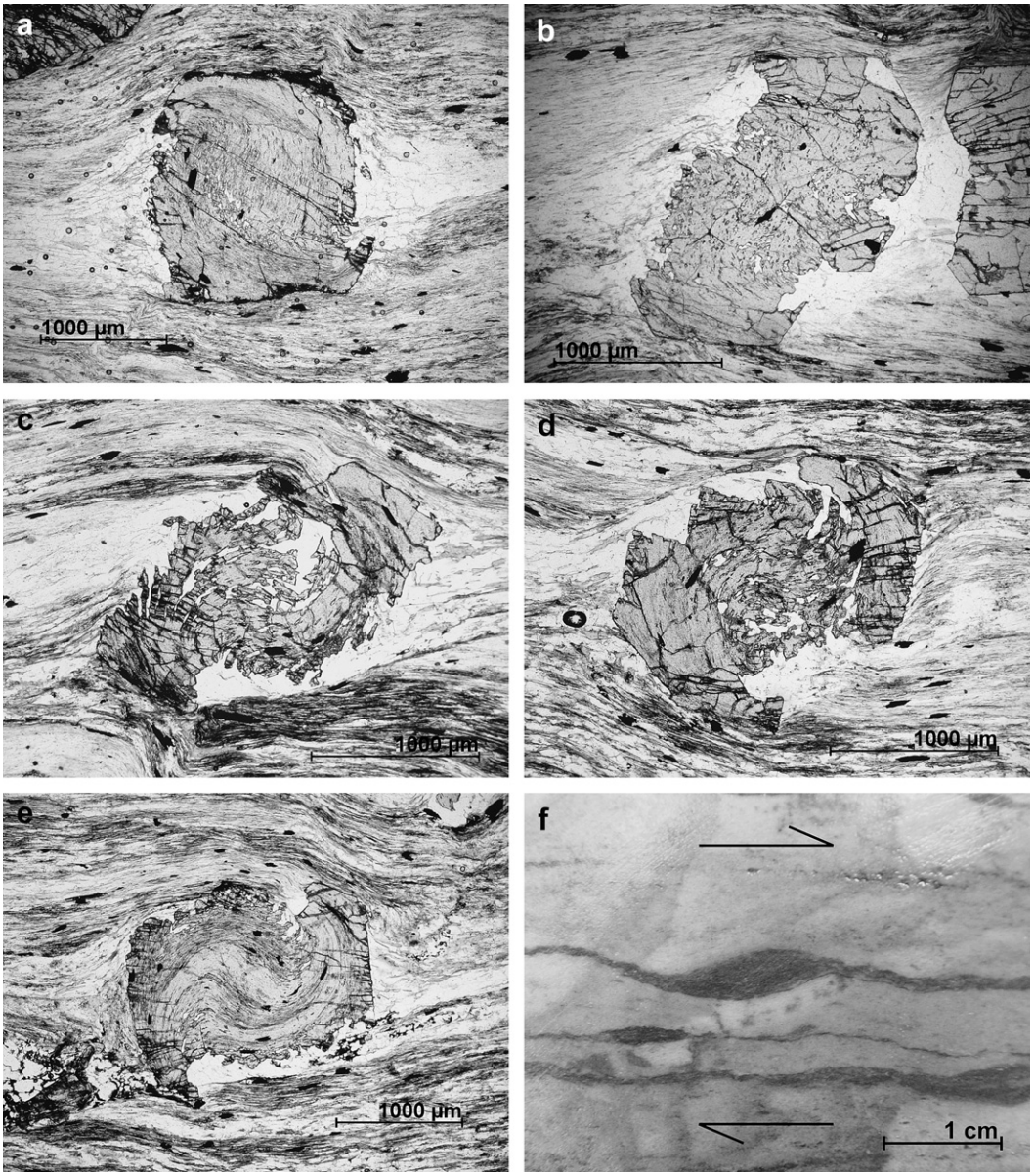

Fig. 3. Garnets with different inclusion trail curvature angles, interpreted to represent different stages of the model presented in Fig. 8. (a) Approximately equidimensional garnet with α of 90°, representing stage 5. (b) Elongated garnet with $\alpha = 135°$, $R = 1.7$ and $\beta = 45°$, representing stage 6. (c) Elongated garnet with $\alpha = 180°$, $R = 1.9$ and $\beta = 20°$, representing a stage between 6 and 7; note D3 crenulation in the lower part. (d) Elongated garnet with $\alpha = 180°$, $R = 1.3$ and $\beta = 20°$, also representing a stage between 6 and 7. (e) Garnet crystal with $\alpha = 220°$, $R = 1.3$ and $\beta = 10°$, representing stage 8. (f) Asymmetric foliation fish, forming an independent shear sense indicator, from the same outcrop as the garnets. The fish indicates a dextral sense of shear in the figure, corresponding to top to the east shear in the outcrop, compatible with the shear sense derived from the garnets, if interpreted as rotational.

more desirable to work with, but the small grain size of the garnets in question (about 1–5 mm) does not permit recognizing the same crystals in different sections. Although this is an obvious drawback in comparing our data with, e.g. those of Johnson (1993a), we believe that the much larger dataset compensates for this.

Of all studied garnets, the maximum curvature angle α between the orientation of the inclusion trails in the centre and the average foliation outside (Fig. 4) was measured. The aspect ratio R between the longest diameter (AB) and the orthogonal shorter one (CD; Fig. 4) was also measured and, finally, the angle β between the longest diameter and the average $S_{1/2}$ in the matrix (Fig. 4).

4.1. Maximum curvature angle (α)

The measured curvature angles (Fig. 5a) show a rather irregular frequency histogram with the main concentration between 90° and 180° and a remarkable peak at 180°. A second high is present at 90°.

We expected a smooth curve reflecting the progressive rotation of spherical objects in a homogeneous flowing matrix, influenced by the cut effect and by the progressive growth effect (Fig. 5b). The cut effect predicts that lateral cuts, away from the core, show less apparent rotation than cuts through the core, simply because these cuts do not attain the oldest parts of the garnets (Powell and Treagus, 1969, 1970). The progressive growth effect takes into account that not all garnets nucleated at the same moment. They grew more probably over a period of time and the younger crystals would consequently show smaller rotation angles than the older ones. Both these effects were expected to produce a number of grains with lower curvature angles (and lower diameter values), more or less as shown in Fig. 5b.

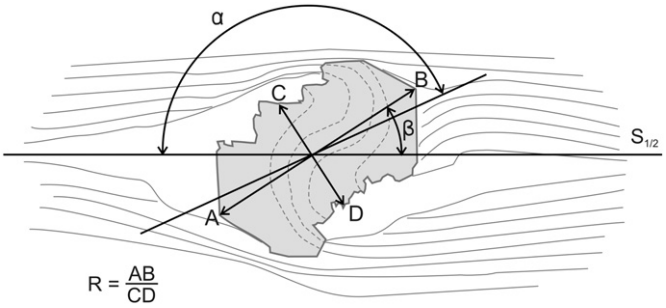

Fig. 4. This figure shows how the inclusion trail curvature angle α was measured, between the tangent of the inclusion trail in the centre of the crystal and the average foliation in the matrix ($S_e = S_{1/2}$); the aspect ratio $R = AB/CD$, and the angle β between the longest dimension of the garnets and the average foliation in the matrix ($S_e = S_{1/2}$).

4.2. Aspect ratio (R)

Although it is assumed in most models that garnets are typically spherical, considerable deviation from sphericity was observed to be more the rule than the exception (Figs. 2, 3, 6a; compare also Johnson, 1993b, his Fig. 3). A comparison between R of garnets with angles α of 90° and 180° (Fig. 6b,c) shows that the former are significantly closer to sphericity (peak of R at 1.2) than the latter (peak of R at 1.4).

4.3. Angle β between the long axis of garnets and the surrounding foliation

The histogram of the angle β (Fig. 7a) shows two peaks: a principal one at 90°, referring to garnets elongated orthogonal to the foliation, and a secondary one at 0°, referring to garnets elongated parallel to the foliation. A third high around 50–60° is also conspicuous. It is striking that no angles between 90° and 180° were observed, meaning that all measured angles are in the "forward rotated" quadrant, in the rotational model.

Comparison of garnets with increasing apparent rotation angles (Fig. 7b) shows that garnets with α around 90° tend to have a high concentration of β around 90° as well, whereas the angle β tends to diminish for garnets with higher rotation angles.

The relation between the size of the garnets and the angle α is shown in Fig. 8. Although there is a rough tendency for larger grains to contain higher α, many crystals with high α are surprisingly small. This probably indicates that the growth rate was not uniform but may be highly influenced by local availability of ions necessary for garnet growth.

Chemical zoning maps for Mn measured in three garnets (Fig. 9) show that the outer parts of elongated garnets, in the direction of their long axis, have lower Mn concentration, suggesting that they represent the latest garnet growth into mica rich strain caps. The inner parts tend to show an oval shape with its long axis at an angle to the long axis of the garnet.

5. Model to interpret the data

The model we propose aims to explain the data presented in the previous section. It is based on the following ideas:

- Although garnets tend to grow approximately spherically, there seems to be a tendency to grow faster into the mica-rich strain caps (Passchier and Trouw, 2005, their Figs. 7.1, 7.32), orthogonal to the surrounding foliation, and slower into the quartz-rich strain shadows, parallel to the foliation (Figs. 2, 3b,c,d, 8; see also Johnson, 1993b, his Fig. 3, in which an elongated shape due to preferential growth into the strain caps is apparent).
- The rotation rate of elongated objects in non-coaxial deformation depends on the aspect ratio, on the vorticity and on the angle between the long axis and the instantaneous stretching axis (ISA) (Marques and Coelho, 2003; Passchier and Trouw, 2005).
- During a period of garnet growth many nuclei may form close to the initiation of this period, but nucleation probably continues during progressive growth of these older crystals to form younger garnets with less rotation.

The succession of eight stages of development as imagined in our model is shown in Fig. 10 and examples of various stages are presented in Figs. 3 and 9.

At stage 1 garnet nucleates syntectonically and starts to overgrow the foliation. Its presence causes a small strain shadow and strain cap due to contemporaneous deformation. Some incipient rotation may occur, but is not shown in the figure for simplifying reasons.

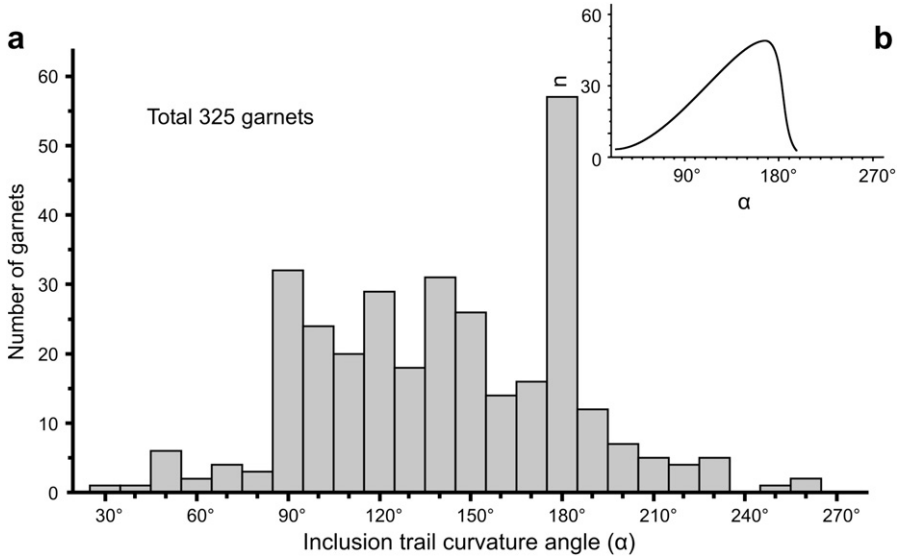

Fig. 5. (a) Histogram of α of all garnets measured. (b) Expected histogram of α according to the rotational model.

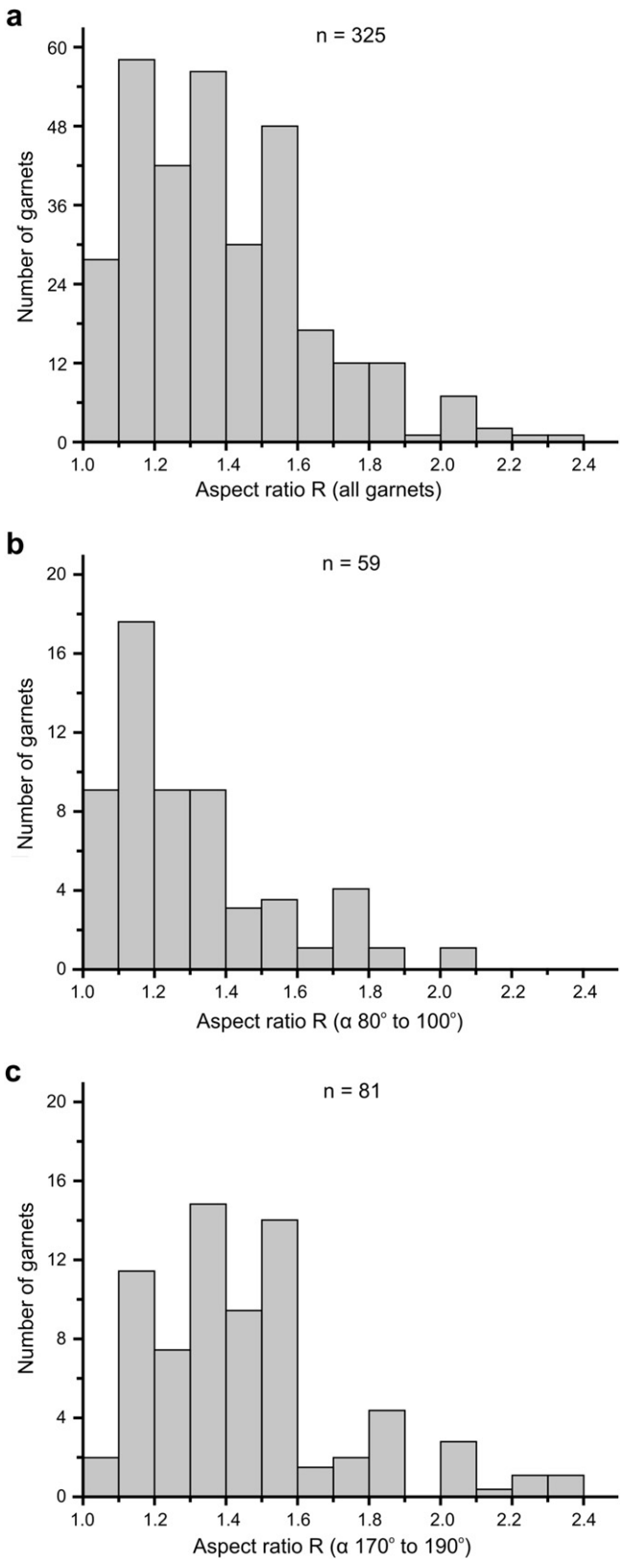

Fig. 6. (a) Histogram of the aspect ratio R of all garnets measured. (b) Same histogram for garnets with α around 90°, and (c) for garnets with α around 180°.

At stage 2 the garnet has grown to a slightly elongated shape, perpendicular to the foliation, due to faster growth into the mica-rich strain caps and slower growth into the quartz-rich strain shadows.

After reaching a certain aspect ratio (possibly around 1.5) the garnet would tend to accelerate its rotation (stage 3) until the long axis reaches a position close to parallel to the foliation. In this position of slow rotation the garnet would show an angle α of about 90° (stage 4).

Continued growth, again preferentially orthogonal to the foliation will first restore an approximately equidimensional shape and eventually produce an elongated shape again, with the long axis perpendicular to the foliation (stage 5; Fig. 3a; an example can also be observed in Passchier and Trouw, 2005, their Fig. 7.32).

When a certain aspect ratio is reached, the garnet would tend to accelerate rotation for another 90° (stages 6 and 7; Fig. 3b,c, 9, BR-2-1), showing now an angle α of about 180°.

At this stage a period of slow rotation would follow (stage 8; Fig. 3d,e, 9, BR-1-16) until the crystals would have grown sufficiently to attain again an elongated shape to accelerate rotation until a position that would show an angle α of about 270°.

In fact there is evidence in our data that a few crystals attained this stage, but a much larger number stopped growing at stage 8, representing the peak of apparent rotation angles at 180° (Fig. 5a). Most of these crystals have an elongated shape ($R = \sim 1.4$, Fig. 6c) with a tendency to be either parallel to the foliation ($\beta = 0$, as at stage 8) or at a moderate angle, that could be explained as asymmetric growth at stages 6 and 7.

The peak frequency of crystals with angles α of about 90° can be explained by the model as representing crystals that nucleated later and are now at stages 4 and/or 5. They are relatively close to an equidimensional shape (Fig. 6b) which can be explained by their intermediate position between stages 4 and 5. Their long axes tend to be at right angles to the foliation (Fig. 7c), showing that most of the crystals were getting closer to stage 5, but did not attain an aspect ratio high enough to enhance accelerated rotation.

The tendency of decreasing β with increasing rotation angle (Fig. 7) can be explained by the model as follows. Many old crystals rotated about 180° and attained a relatively stable position with β close to zero. Other younger crystals rotated 90° or values intermediate between 90° and 180° and exhibit higher β values, especially the ones with rotation around 90°, because they were growing perpendicular to the foliation but did not reach a high enough aspect ratio before the growing process and the tectonic movements stopped.

The examples shown in Fig. 9 illustrate the progressive growth of three garnets compatible with the model. The garnet BR-2-1 (Fig. 9) with α of about 150° represents stage 6 of the model. The blue upper and lower parts reflect clearly the latest growth into the strain caps as visualized in stage 5. Garnet BR-1-16 (Fig. 9) with α of 180° is intermediate between stages 7 and 8 with somewhat asymmetric growth into the strain caps, and garnet BR-1-27 with α of 225° represents a stage slightly more advanced than stage 8 with an extra 45° of rotation. This last garnet shows a reddish core (Fig. 9) with higher Mn with an oval shape almost at right angles to the long axis of the crystal, as predicted in the model.

6. Discussion

The model proposed here is thought to function in addition to the classical rotational models for spherical crystals as proposed by, e.g. Schoneveld (1977); see also Masuda and Mochizuki (1989); and discussed by Johnson (1993a, 1999a). It merely adds details, especially for non-spherical crystals, explaining the observed deviation from the expected frequency distribution curve for inclusion trail curvature angles. An important fact is that no angles β in the quadrant 90–180° were observed. This means that all elongated crystals are in such a position that their long axis is in the "foreward rotated" quadrant according to the rotational model (compare also Johnson, 1993b, his Fig. 3).

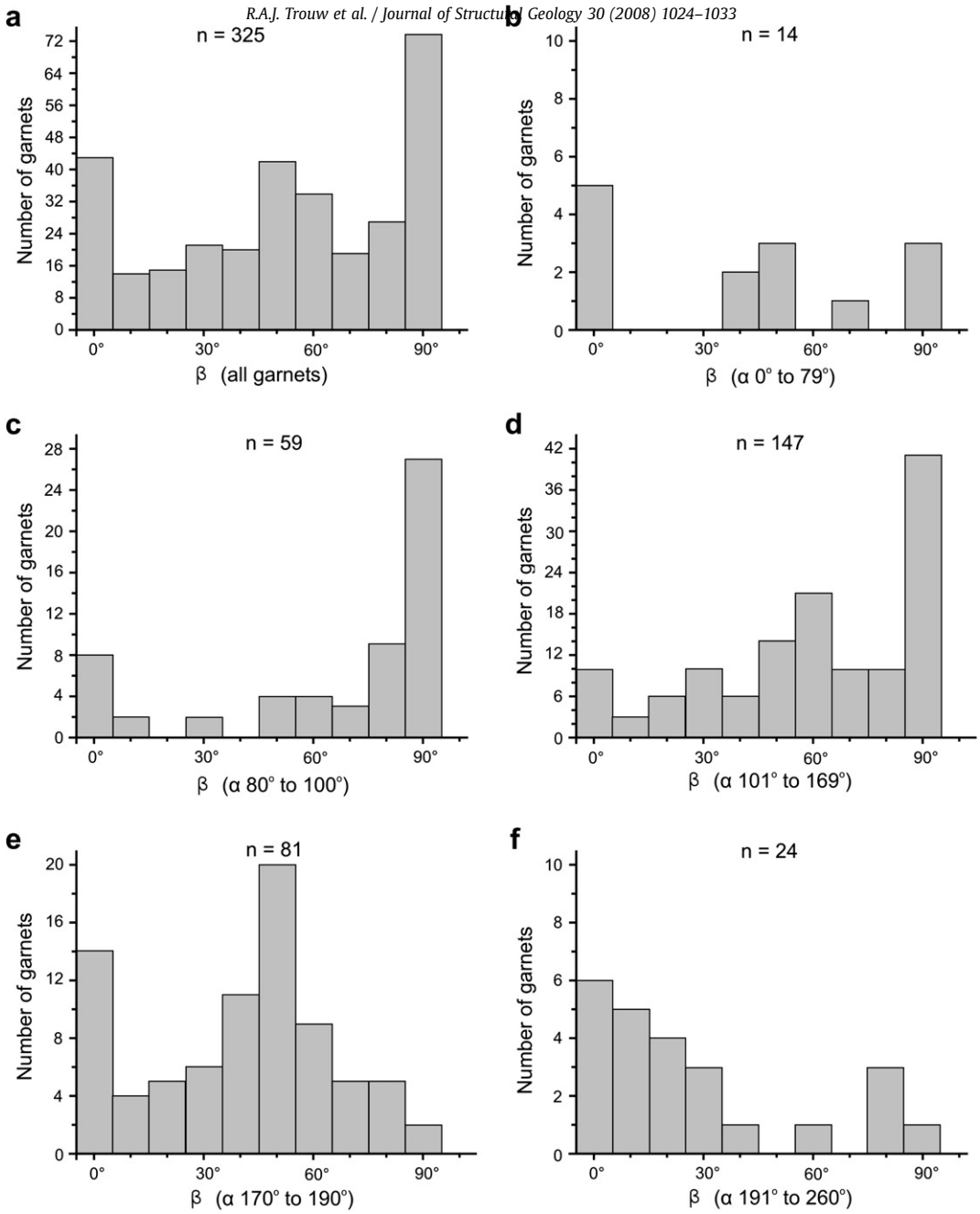

Fig. 7. (a) Histogram of the angle β of all garnets measured; (b) β of garnets with α 0–79°; (c) β of garnets with α between 80° and 100°; (d) β of garnets with α between 101° and 169°; (e) β of garnets with α between 170° and 190°; (f) β of garnets with α between 191° and 260°.

This, in our view, if compared with the position of elongated fish shaped crystals with positive stair stepping (e.g. Pennacchioni et al., 2001; Mancktelow et al., 2002; ten Grotenhuis et al., 2002, 2003), is in itself a strong argument in favor of the rotational model and also in favor of the model proposed here. Masuda et al. (1995) predicted that a stable position of elongated objects in non-coaxial deformation could be reached with beta in the range 90–180°, that is in the "backwards rotated" quadrant. However, it has to be realized that there are several important differences between the model proposed here and the one published by Masuda et al. (1995); see also Passchier (1987). We do not propose that our garnets reached a stable position in a strong rotational flow. The highest rotation angle measured of about 250° means that this garnet did not complete one full revolution around its axis during its complete growth period. Snowball garnets are usually reported from schists, not from mylonites, where the growth rate kept pace with the strain rate. Also, our R

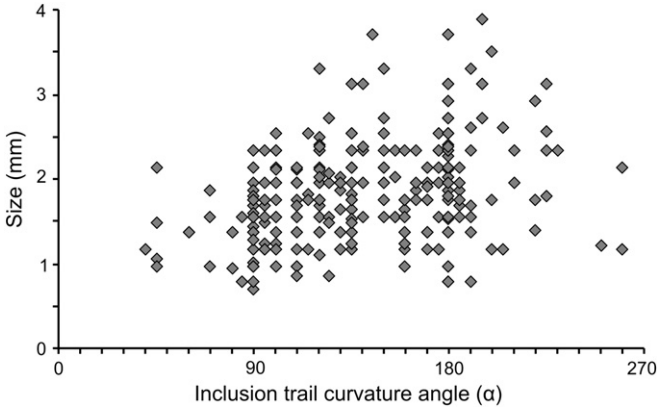

Fig. 8. Relation of garnet size versus α.

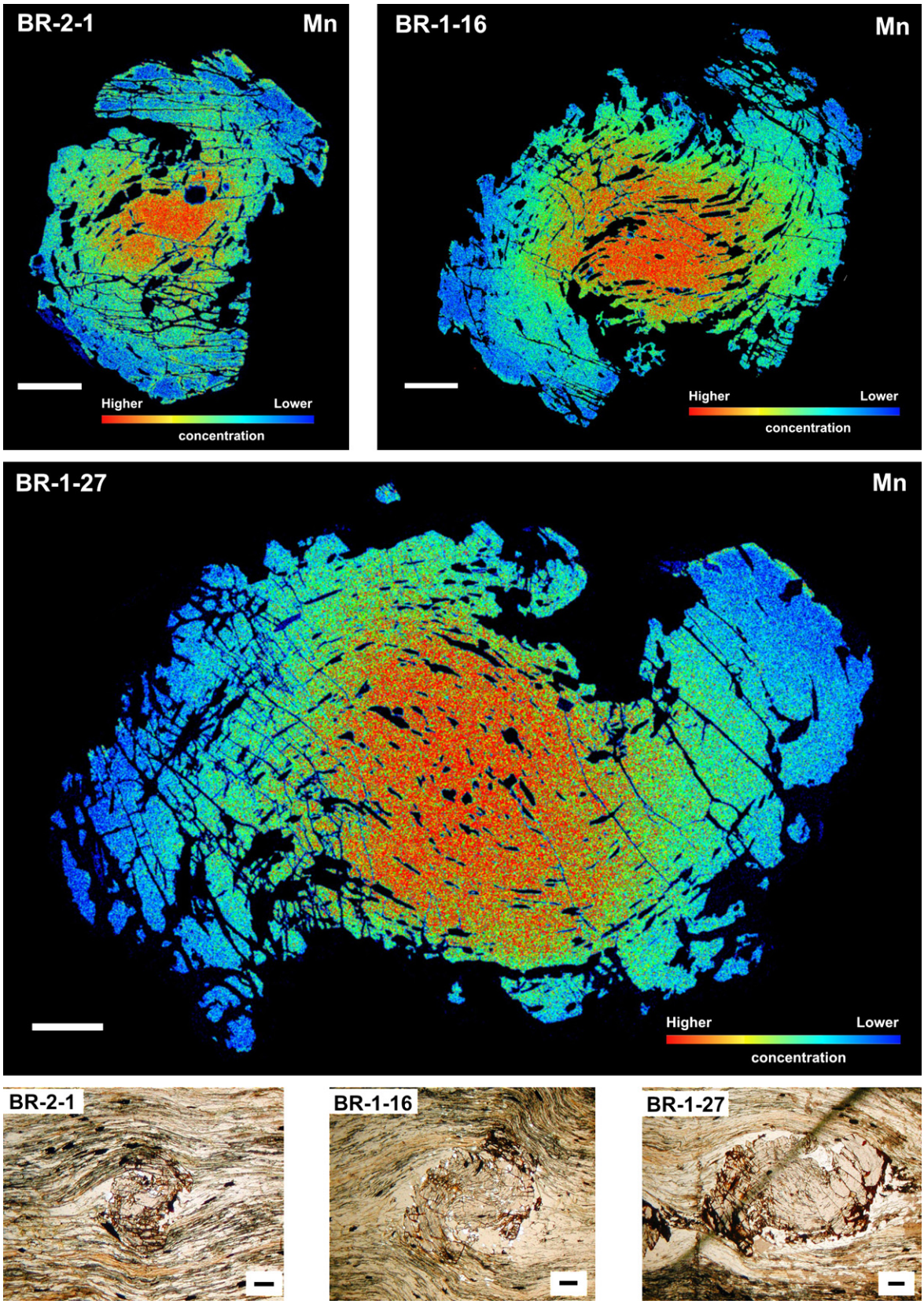

Fig. 9. Chemical zoning maps showing the variation in percentage of Mn in three garnets, BR-2-1, BR-1-16 and BR-1-27. The same garnets are also shown in plane polarized light with their surrounding S_e at the bottom of the figure. All scale bars represent 0.2 mm. The α values of the three garnets are respectively 150°, 180° and 225°. Note that the red central part of the garnets tends to show an oval shape with its long axis at an angle to the long axis of the garnet.

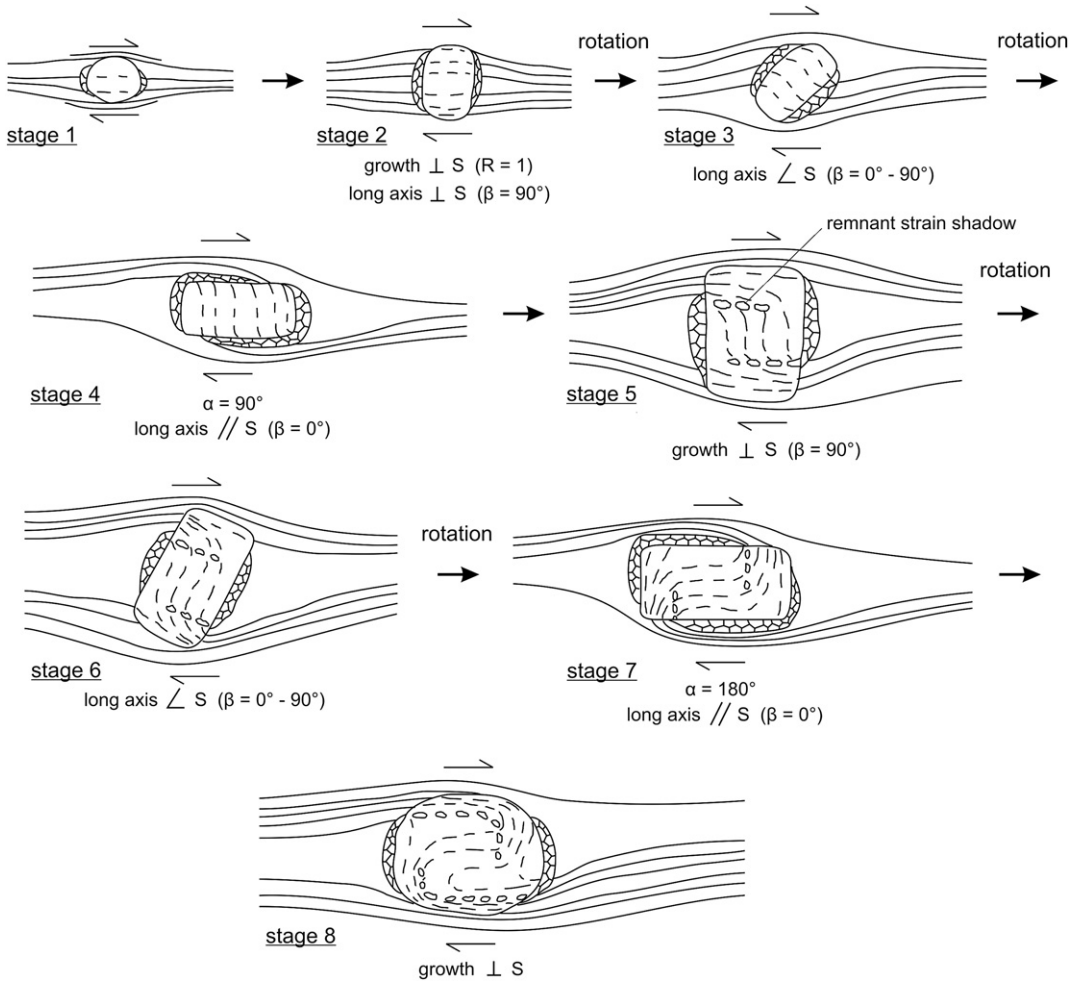

Fig. 10. Eight stages of the evolutionary model proposed to explain the concentrations of α in multiples of 90°. See text for further explanation.

values are far too low to reach the stable positions predicted by Masuda et al. (1995).

In the non-rotational model, where the shear sense in the matrix would be opposite, this orientation of the elongated grains seems to be difficult to explain.

We conclude that our measurements can be satisfactorily explained by the model we propose. The model is based on the ideas of rotation of spherical and elongated objects in a flowing matrix. Although garnets are generally thought of as spherical, under specific circumstances, they could become elongated by preferential growth into their strain caps, orthogonal to the foliation.

Spherical objects would rotate at a constant rate whereas elongated objects would rotate at a variable rate according to their position. This variable rotation rate would cause, at any stage, a tendency to produce frequency peaks around 90°, 180°, 270° etc.

Independent from the model proposed above we would like to discuss several other points related to the rotational and non-rotational models.

The first point is that spiral shaped inclusion trails with curvature angles in excess of 180° are only reported in garnet porphyroblasts (Rosenfeld, 1970; Schoneveld, 1977; Vernon, 1978) that, because of their cubic crystal habit tend to be approximately spherical or equidimensional in shape. They have not been described in staurolite, kyanite, chloritoid, biotite, andalusite etc. that are usually more elongated in shape. The rotational model explains this fact satisfactorily since it is based on the continuous rotation of a growing sphere. The non-rotational model, based on rotation of matrix around stable porphyroblasts is independent of the shape of the porphyroblasts and therefore fails to explain the relation between approximately spherical garnets and high curvature angles.

One could argue that the model proposed above is in disagreement with this line of thought since it emphasizes the deviation from sphericity in garnets. However, this deviation is only temporary and tends to be restored by growth in orthogonal directions, which is easy in cubic garnets but not probable in non-cubic minerals.

Another point in favor of rotation is the large number of successive deformation phases, all simultaneous with garnet growth, required in the non-rotational model to obtain curvature angles in excess of 180°. In the areas we are familiar with and that contain garnets with spiral shaped inclusion trails, not more than three or four regional deformation phases were recognized and usually only one or two are contemporaneous with garnet growth (in the case described above D_1 and D_2). If the non-rotational model would be correct in these areas then the record of at least three or four deformational phases would have been completely erased. This seems highly unlikely to us, since most deformation phases are strongly or weakly developed in certain areas or certain lithotypes, permitting their recognition at least somewhere, independent from the garnets.

A third point is related to the sequence of events during the progressive development of a crenulation cleavage as first proposed by Bell and Rubenach (1983). The non-rotational model is largely based on successive repetitions of this scheme of events in metamorphic rocks during garnet growth. A slightly modified version of

this scheme is presented in Passchier and Trouw (2005, their Figs. 4.18 and 4.19). We would like to call attention to the fact that in our experience the final stage as depicted in both schemes is rarely exactly identical to the first stage; the matrix tends to be coarser because the complete erasure of crenulation hinges (between stages 4 and 5 in both schemes) requires considerable grain growth of micas as, e.g. depicted in Passchier and Trouw (2005, their Fig. 4.28). This grain growth will in our opinion rarely produce a new fabric with the same grain size as the previous one. Since garnets tend to grow during progressively increasing metamorphic conditions, the new fabric would tend to be coarser than the previous one. This progressive coarsening of the matrix during garnet growth would, in our opinion, be required in the non-rotational model to explain the complete erasure of several crenulation cleavages. However, in the cases described above and the ones illustrated in Johnson (1993a,b) no such coarsening is apparent.

A final point that needs attention is related to the idea that growth and deformation rates are continuous in time. Our model (as the model proposed by Schoneveld, 1977) is roughly based on this idea, but it is not dependent on it. The size versus alpha graph (Fig. 8) shows that growth rate is probably not constant, and grains may grow during the same period to different sizes, possibly related to availability of ions in the vicinity. This, however, does not invalidate the model proposed here. If growth or deformation are pulsating in time, the effect of clustering of curvature angles around multiples of 90° would be even more enhanced.

A final remark is that we are of the opinion that the arguments in favor of rotational or non-rotational models should be discussed in their geological context.

Acknowledgements

André Ribeiro is gratefully acknowledged for the mapping and discovery of the outcrop explored in this paper. The two first authors acknowledge financial support from CNPq (Brazilian National Research Agency).

References

Bell, T.H., Johnson, S.E., 1989. Porphyroblast intrusion trails: the key to orogenesis. Journal of Metamorphic Geology 3, 109–118.

Bell, T.H., Rubenach, M.J., 1983. Sequential porphyroblast growth and crenulation cleavage development during progressive deformation. Tectonophysics 92, 171–194.

Campos Neto, M.C., Caby, R., 1999. Neoproterozoic high-pressure metamorphism and tectonic constraint from nappe system south of the São Francisco craton, southeast Brazil. Precambrian Research 97, 3–26.

Campos Neto, M.C., Caby, R., 2000. Lower crust extrusion and terrane accretion in the Neoproterozoic nappes of southeast Brazil. Tectonics 19, 669–687.

ten Grotenhuis, S.M., Passchier, C.W., Bons, P.D., 2002. The influence of strain localisation on the rotation behaviour of rigid objects in experimental shear zones. Journal of Structural Geology 24, 485–501.

ten Grotenhuis, S.M., Trouw, R.A.J., Passchier, C.W., 2003. Evolution of mica fish in mylonitic rocks. Tectonophysics 372, 1–21.

Jiang, D., 2001. Reading history of folding from porphyroblasts. Journal of Structural Geology 23, 1327–1335.

Jiang, D., Williams, P.F., 2004. Reference frame, angular momentum, and porphyroblast rotation. Journal of Structural Geology 26, 2211–2224.

Johnson, S.E., 1993a. Testing models for the development of spiral-shaped inclusion trails in garnet porphyroblasts: to rotate or not to rotate, that is the question. Journal of Metamorphic Geology 11, 635–659.

Johnson, S.E., 1993b. Unravelling the spirals: a serial thin-section study and three-dimensional computer-aided reconstruction of spiral-shaped inclusion trails in garnet porphyroblasts. Journal of Metamorphic Geology 11, 621–634.

Johnson, S.E., 1999a. Near-orthogonal foliation development in orogens: meaningless complexity, or reflection of fundamental dynamic processes? Journal of Structural Geology 21, 1183–1187.

Johnson, S.E., 1999b. Porphyroblast microstructures; a review of current and future trends. American Mineralogist 84, 1711–1726.

Mancktelow, N.S., Arbaret, L., Pennacchioni, G., 2002. Experimental observations on the effect of interface slip on rotation and stabilisation of rigid particles in simple shear and a comparison with natural mylonites. Journal of Structural Geology 24, 567–585.

Marques, F.O., Coelho, S., 2003. 2-D shape preferred orientations of rigid particles in transtensional viscous flow. Journal of Structural Geology 25, 841–854.

Masuda, T., Mochizuki, S., 1989. Development of snowball structure: numerical simulation of inclusion trails during synkinematic porphyroblast growth in metamorphic rocks. Tectonophysics 170, 141–150.

Masuda, T., Michibayashi, K., Ohta, H., 1995. Shape preferred orientation of rigid particles in a viscous matrix: re-evaluation to determine kinematic parameters of ductile deformation. Journal of Structural Geology 17, 115–129.

Paciullo, F.V.P., Ribeiro, A., Andreis, R.R., 2000. The Andrelândia basin, a Neoproterozoic intraplate continental margin, southern Brasilia belt. Revista Brasileira de Geociências 30, 200–202.

Passchier, C.W., 1987. Stable positions of rigid objects in non-coaxial flow: a study in vorticity analysis. Journal of Structural Geology 9, 679–690.

Passchier, C.W., Trouw, R.A.J., 2005. Microtectonics. Springer Verlag.

Pennacchioni, G., Di Toro, G., Mancktelow, N.S., 2001. Strain-insensitive preferred orientation of porphyroclasts in Mont Mary mylonites. Journal of Structural Geology 23, 1281–1298.

Powell, D., Treagus, J.E., 1969. On the geometry of S-shaped inclusion trails in garnet porphyroblasts. Mineralogical Magazine 36, 453–456.

Powell, D., Treagus, J.E., 1970. Rotational fabrics in metamorphic minerals. Mineralogical Magazine 37, 801–814.

Rosenfeld, J.L., 1970. Rotated garnets in metamorphic rocks. In: Special Paper No. 129. Geological Society, America. 102pp.

Schoneveld, C., 1977. A study of some typical inclusion patterns in strongly paracrystalline rotated garnets. Tectonophysics 39, 453–471.

Trouw, R.A.J., Heilbron, M., Ribeiro, A., Paciullo, F., Valeriano, C.M., Almeida, J.C.H., Tupinambá, M., Andreis, R.R., 2000. The central segment of the Ribeira belt, in: Tectonic Evolution of South America. 31st International Geological Congress, Rio de Janeiro, pp. 287-310.

Vernon, R.H., 1978. Porphyroblast-matrix microstructural relationships in deformed metamorphic rocks. Geologische Rundschau 67, 288–305.

Williams, P.F., Jiang, D., 1999. Rotating garnets. Journal of Metamorphic Geology 17, 367–378.